Supplementary Information for

The conformation and orientational order of a 1,2-disubstituted ethane nematogenic molecule (I22) in liquid crystalline and isotropic phases studied by NMR spectroscopy

by

James W. Emsley[1*], Philippe Lesot[2], Anne Lesage[3], Giuseppina De Luca[4], Denis Merlet[2]

and Giuseppe Pileio[1]

1. School of Chemistry, University of Southampton, Southampton, SO17 1BJ, UK.
2. Laboratoire de Chimie Structurale Organique, RMN en Milieu Orienté, Université Paris-Sud 11, ICMMO, UMR CNRS 8182, Bât. 410, F-91405 Orsay cedex, France.
3. Université de Lyon, CNRS/ ENS Lyon/ UCB-Lyon 1, Centre RMN à Très Hauts Champs, 5 rue de la Doua, 69100 Villeurbanne, France.
4. Dipartimento di Chimica, Universita della Calabria, 87030 Arcavacata di Rende, Italy.
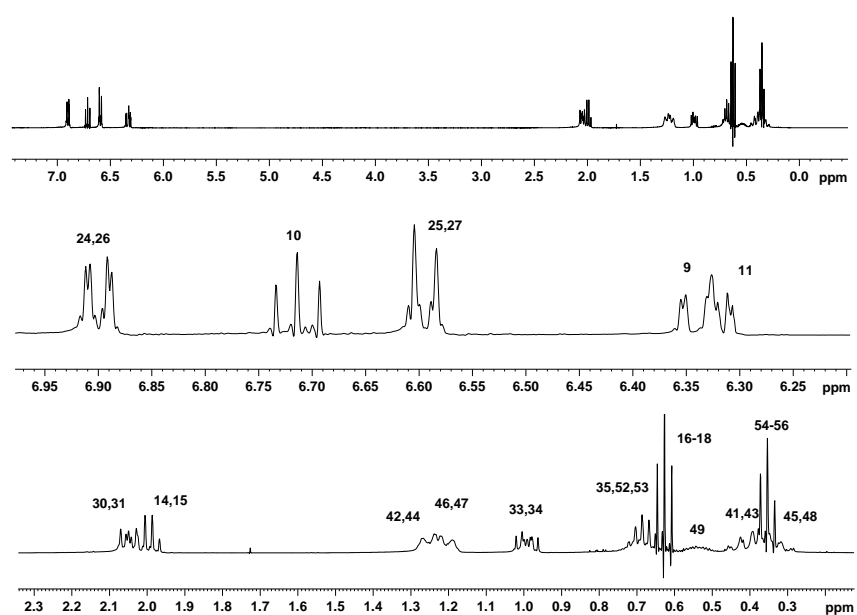
Figure S1. 400 MHz ^{1}H spectrum of a sample of **I22** in the isotropic phase at 373 K. The spectrum is the result of Fourier transforming 16 free induction decays using 16K data points. Gaussian apodisation was applied.
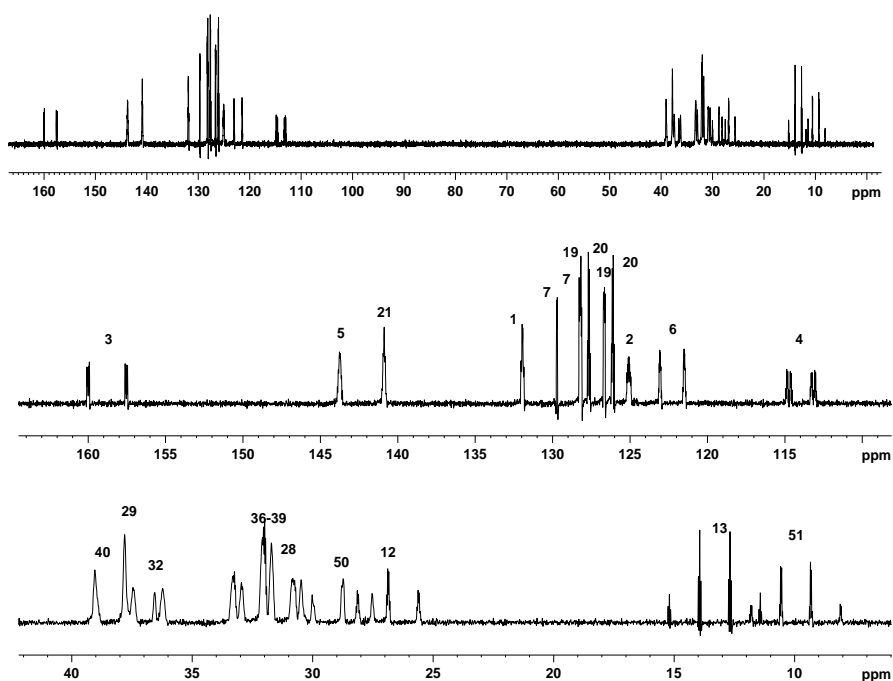
Figure S2. 100 MHz ^{13}C spectrum of a sample of **I22** in the isotropic phase at 373 K. The spectrum is the result of Fourier transforming 2048 free induction decays using 16K data points. A zero filling to 64K data points and a Gaussian apodisation was applied prior to Fourier transformation.

Table S1. The bond lengths, r_{ij}, the bond angles, θ_{ijk}, and dihedral angles, ϕ_{ijks}, of **I22** calculated by the DFT method B3LYP/6-31G*.

i	j	r_{ij} /Å	k	θ_{ijk} /°	s	ϕ_{ijks} /°
2	1	1.484				
3	2	1.402	1	123.05		
4	3	1.388	2	123.30	1	179.08
5	4	1.399	3	120.23	2	-0.06
6	5	1.401	4	117.81	3	0.19
7	2	1.406	3	115.53	4	-0.13
8	3	1.355	2	119.40	1	-0.46
9	4	1.086	3	118.45	2	180.19
10	7	1.086	2	118.43	1	2.55
11	6	1.087	5	119.54	4	179.03
12	5	1.514	4	120.83	3	181.83
13	12	1.540	5	112.81	4	88.33
14	12	1.097	5	109.38	13	121.70
15	12	1.097	5	109.60	13	-121.86
16	13	1.096	12	110.85	5	179.89
17	13	1.096	12	111.01	5	-59.94
18	13	1.096	12	110.98	5	59.71
19	1	1.405	2	121.97	3	40.57
20	19	1.392	1	120.84	2	178.81
21	20	1.401	19	121.47	1	0.33
22	21	1.400	20	117.64	19	-0.37
23	22	1.393	21	121.20	20	0.26
24	19	1.084	1	119.64	2	-0.60
25	20	1.088	19	119.18	1	180.56
26	23	1.087	1	119.46	2	2.34
27	22	1.088	21	119.45	20	179.79
28	21	1.513	20	121.02	19	177.25
29	28	1.544	21	112.34	20	-86.22
30	28	1.098	21	109.60	29	121.15
31	28	1.097	21	109.43	29	-122.28
32	29	1.540	28	115.20	21	175.16
33	29	1.100	28	108.99	32	123.46
34	29	1.099	28	108.21	32	-121.85
35	32	1.103	29	107.78	33	182.20
36	32	1.541	29	113.32	35	118.91
37	32	1.541	29	110.58	35	-117.19
38	36	1.538	32	112.25	37	53.80
39	37	1.536	32	112.53	36	-54.03
40	38	1.540	36	112.04	32	-55.71
41	36	1.101	32	108.78	35	176.02
42	36	1.097	32	110.49	35	59.56
43	37	1.101	32	108.84	35	183.99
44	37	1.098	32	109.70	35	-60.10

45	38	1.101	36	108.88	32	65.69
46	38	1.099	36	109.85	32	181.82
47	39	1.099	37	109.96	32	178.22
48	39	1.100	37	108.92	32	-65.54
49	40	1.103	38	106.80	36	-60.28
50	40	1.540	38	113.35	36	179.89
51	50	1.533	40	116.40	38	171.70
52	50	1.100	40	108.97	51	123.25
53	50	1.099	40	108.40	51	-121.92
54	51	1.096	50	110.92	40	183.21
55	51	1.097	50	111.11	54	119.61
56	51	1.097	50	112.06	54	-119.94

Table S2. The local interaction parameters, $\varepsilon_{ij}(ring1,N)$ /RT, the bond lengths, r_{ij} /Å, and bond angles. θ_{ijk} /° obtained by fitting calculated to observed dipolar couplings within the fluorinated aromatic ring in **I22** when the sample is in the nematic phase at 293 K. The bond lengths and angles optimised for the non-fluorinated ring are also given.

Interaction parameters /RT

ε_{12}	*(ring1,N)*	3.72 ± 0.090
$\varepsilon_{3,7}(ring1,N)$		0.055 ± 0.025
$\varepsilon_{3,8}(ring1,N)$		0.045 ± 0.051

Geometrical parameters

$r_{3,8} =$	1.393 ± 0.016
$r_{6,11} =$	1.097 ± 0.013
$r_{7,10} =$	1.071 ± 0.010
$r_{19,24} = r_{23,26}$	1.073 ± 0.009
$r_{20,25} = r_{22,27}$	1.074 ± 0.016
$\theta_{8,3,2}$	119.9 ± 0.5
$\theta_{9,4,3}$	119.6 ± 0.3
$\theta_{11,6,5}$	119.9 ± 0.5
$\theta_{10,7,2}$	117.3 ± 0.4
$\theta_{24,19,1} = \theta_{26,23,1}$	119.5 ± 0.1

Table S3. Local interaction parameters obtained for the fluorinated ring in **I22** in the chiral nematic phase, $\varepsilon_{ij}(ring1,Ch)$, and in the isotropic phase, $\varepsilon_{ij}(ring1,iso)$.

$\varepsilon_{1,2}(ring1,Ch)/RT$	$\varepsilon_{3,7}(ring1,Ch)/RT$	$\varepsilon_{3,8}(ring1,Ch)/RT$
0.097 ± 0.004	-0.011 ± 0.007	0.007 ± 0.004
$\varepsilon_{1,2}(ring1,iso)/RT$	$\varepsilon_{3,7}(ring1,iso)/RT$	$\varepsilon_{3,8}(ring1,iso)/RT$
0.097 ± 0.004	-0.011 ± 0.007	0.007 ± 0.004

Table S4. The local interaction, $\varepsilon_{i,j}(ring\text{-}ethyl,N)/RT$, and geometrical parameters for the ring-ethyl fragment of **I22** obtained by fitting calculated to observed residual dipolar couplings for the nematic phase at 293 K.

Interaction parameters

$\varepsilon_{1,2}(ring\text{-}ethyl,N)/RT$	3.53 ± 0.02
$\varepsilon_{5,13}(ring\text{-}ethyl,N)/RT$	0.87 ± 0.04
$\varepsilon_{14,15}(ring\text{-}ethyl,N)/RT$	0.67 ± 0.2
$\varepsilon_{3,8}(ring\text{-}ethyl,N)/RT$	-0.02 ± 0.03

Geometric parameters

$\theta_{5,12,13} / °$	115.7 ± 0.2
$\theta_{14,12,5} / °$	109.6 ± 0.1
$\delta_{14,12,5,13} / °$	119.6 ± 0.1

Table S5. The local interaction coefficients, $\varepsilon_{ij}(ethane1,N)/RT$, and the geometrical parameters obtained by fitting calculated to observed residual dipolar couplings to the rigid fragment ethane1 of **I22** in the nematic phase.

$r_{28,30} = r_{28,31} /Å$	1.111
$\theta_{30,28,21} = \theta_{31,28,21} /°$	111.2
$\varepsilon_{21,26}(ethane1,N)/RT$	4.58
$\varepsilon_{21,27}(ethane1,N)/RT$	2.42
$\varepsilon_{30,31}(ethane1,N)/RT$	3.46

Table S6. The local interaction coefficients, $\varepsilon_{ij}(ethane2,N)/RT$ obtained by fitting calculated to observed residual dipolar couplings to the rigid fragment ethane2 of **I22** in the nematic phase.

$\varepsilon_{21,28}(ethane2,N)/RT$	3.74 ± 0.04
$\varepsilon_{21,29}(ethane2,N)/RT$	1.6 ± 0.5
$\varepsilon_{30,31}(ethane2,N)/RT$	0.95 ± 0.03
$\varepsilon_{28,32}(ethane2,N)/RT$	0.48 ± 0.53

**Table S7**. The local interaction coefficients, $\varepsilon_{ij}(cyclo,N)/RT$, and the geometrical parameters obtained by fitting calculated to observed residual dipolar couplings for the rigid cyclohexane fragment in the nematic phase at 293 K.

$r_{36,41} = r_{37,43}$	1.106 ± 0.001 Å
$r_{36,42} = r_{37,44}$	1.108 ± 0.009 Å
$r_{38,45} = r_{39,48}$	1.108 ± 0.001 Å
$r_{38,46} = r_{39,47}$	1.097 ± 0.009 Å
$r_{40,49}$	1.104 ± 0.001 Å
$\delta_{49,40,38,36}$	$-64.2°$
$\varepsilon_{29,32}(cyclo,N)/RT$	0.4 ± 0.1
$\varepsilon_{32,35}(cyclo,N)/RT$	-2.83 ± 0.06
$\varepsilon_{36,37}(cyclo,N)/RT$	-4.6 ± 0.5

Table S8.   The local interaction coefficients, $\varepsilon_{ij}(cyclo\text{-}ethane,N)/RT$ obtained by fitting calculated to observed residual dipolar couplings to the cyclohexyl-ethane fragment of **I22** in the nematic phase at 293 K.

$\varepsilon_{21,28}(cyclo\text{-}ethane,N)$	1.24 ± 0.08
$\varepsilon_{21,29}(cyclo\text{-}ethane,N)$	0.6 ± 0.1
$\varepsilon_{30,31}(cyclo\text{-}ethane,N)$	1.3 ± 0.2
$\varepsilon_{33,34}(cyclo\text{-}ethane,N)$	-2.71 ± 0.03
$\varepsilon_{28,32}(cyclo\text{-}ethane,N)$	-4.5 ± 0.1

Table S9.   The local interaction coefficients, $\varepsilon_{ij}(cyclo\text{-}ethyl,N)/RT$ obtained by fitting calculated to observed residual dipolar couplings to the fragment of **I22** in the nematic phase.
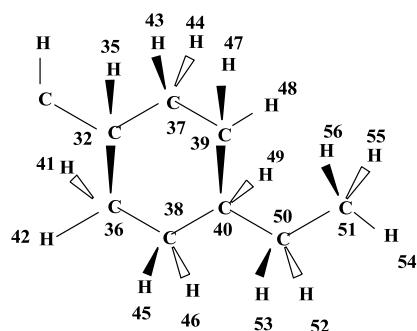
$\varepsilon_{29,32}(cyclo\text{-}ethyl,N)$	2.0 ± 0.3
$\varepsilon_{32,35}(cyclo\text{-}ethyl,N)$	-1.93 ± 0.06
$\varepsilon_{36,37}(cyclo\text{-}ethyl,N)$	-3.5 ± 0.1
$\varepsilon_{40,51}(cyclo\text{-}ethyl,N)$	1.6 ± 0.3
$\varepsilon_{52,53}(cyclo\text{-}ethyl,N)$	2.7 ± 0.5
$\theta_{50,40,38}$ /°	$115. \pm 1$
$\theta_{51,50,40}$ /°	117.9 ± 0.1